

Development of a Laser Ranging Target Optimized for LEO Spacecraft

by

James A. Georges III, G. Charmaine Gilbreath, Peter B. Rolsma¹, Robert A Kessel
U. S. Naval Research Laboratory
Washington DC, 20375

ABSTRACT

A retroreflector array was designed at the Naval Research Laboratory for Low Earth Orbit spacecraft. The size and type of retroreflectors used and their specific orientations on the physical array were mathematically modeled. The array itself was characterized in the laboratory and results were compared with theory. Using these results, a link analysis was then performed to predict the number of photoelectrons that would be received over Capraia using the Field Transportable Laser Radar System for high and low TOPEX passes.

I. Introduction

This paper describes a retroreflector array designed at the Naval Research Laboratory (NRL) for Low Earth Orbit (LEO) spacecraft [1]. The objective of this design is to produce a lightweight and compact retroreflector array with a Laser Radar Cross Section (LRCS) of at least 10^4 square meters above 20° elevation, for a circular orbit. Modeling indicated that an array of one-centimeter diameter retroreflectors would provide the Far Field Diffraction Pattern (FFDP) required to close the link for the orbits of interest. The array itself was characterized in the laboratory and results are summarized in the paper. Modeled results are compared with measurements and implications for link closure are made as well. Specifically, the Number of Photoelectrons (Npe) received over Capraia using the Field Transportable Laser Radar Station (FTLRS) system were predicted for the array for high and low TOPEX passes [2].

The NRL LEO retroreflector array integrates 22 one-centimeter diameter fused silica retroreflectors onto a hemisphere 43mm in height and 82mm in diameter and is 221 grams. The array was then space-qualified in terms of thermal, shock, and vibration at NRL. The array is shown in Figure 1.

¹Peter Rolsma is now with Stanford Telecom, Ashburn, VA, 20147.

II. Model Considerations

The NRL LEO retroarray was designed based on mathematical modeling that incorporated the predicted Far Field Diffraction Pattern for a given design with the velocity aberration produced by an orbit's characteristics.

Due to the finite aperture size of the array and range to a given LEO spacecraft, the spatial distribution of the return pulse is the aperture's Far Field Diffraction Pattern. The purpose of considering an array of smaller cubes is to reduce the impact of velocity aberration on predicted returns. For example, velocity aberration when expressed as an angle falls in the range of 39 to 50 μrad which is typical for a LEO spacecraft with altitudes of 1000 km to 1350 km. A one-centimeter aperture diffracts more strongly than a 2.54 cm aperture and distributes the FFDP into larger angles. Hence, for a LEO spacecraft in the range of interest, the ground receive site will be located within the main intensity lobe of a single 1-centimeter cube but in the third lobe and on a steep slope for a single 2.54 cm aperture. This point is illustrated in Figure 2.

It can be seen in the figure that the velocity aberration induced variations in LRCS are mitigated for a given orbit with the 1-cm cube; however, the value itself does not meet the 10^4 squared meter criteria. Therefore, an array is required to increase the predicted return. Atmospheric-induced averaging enables modeling of the incoherent sum of a candidate array. The development of the incoherent sum as presented in [1] begins with the coherent sum

$$\tilde{a} = \sum_{l=1}^L \tilde{a}_l e^{i\alpha_l} \quad (1)$$

where the α 's are the phase angles for each retroreflector and \tilde{a}_l is the FFDP of a given aperture. The relationship between the instantaneous FFDP and LRCS is:

$$\sigma_{LRCS} = \rho \frac{4\pi}{\lambda^2} |\tilde{a}\tilde{a}^*| \quad (2)$$

where σ_{LRCS} is the Laser Radar Cross Section, ρ is the reflectivity and λ is the wavelength of light. Substitution yields:

$$\sigma_{LRCS} = \rho \frac{4\pi}{\lambda^2} \left| \left(\sum_{m=1}^L \tilde{a}_m e^{i\alpha_m} \right) \left(\sum_{n=1}^L \tilde{a}_n^* e^{-i\alpha_n} \right) \right| \quad (3)$$

$$= \rho \frac{4\pi}{\lambda^2} \left| \sum_{m=1}^L \sum_{n=1}^L \tilde{a}_m \tilde{a}_n^* e^{i(\alpha_m - \alpha_n)} \right| \quad (4)$$

During the interval, τ , variations of phase angle between individual retroreflectors can occur. Provided the statistical correlation between α_m and α_n over τ is small, the resulting phase factors can be treated as essentially random fluctuations. As atmospheric fluctuations are on the order of milliseconds, this condition is met. Consequently, the time-averaged LRCS will simplify to:

$$\overline{\sigma_{LRCS}} = \rho \frac{4\pi}{\lambda^2} \left| \sum_{m=1}^L \sum_{n=1}^L \frac{a_m a_n^*}{\tau} \int_0^\tau e^{i(\alpha(t)_m - \alpha(t)_n)} dt \right| \quad (5)$$

$$= \rho \frac{4\pi}{\lambda^2} \sum_{m=1}^L |\tilde{a}_m|^2 \quad (6)$$

Considerations for bevel thickness, depth of recess into array, and index of refraction were also included. A LRCS distribution for the time-averaged response at 532 nm with 2.032 cm bevels for fused silica retroreflectors is shown in Figure 3.

III. Experimental Verification

The performance of the array was characterized in a compact far field optical test bed as shown in Figure 4. The light from an argon-ion laser operating at 514 nm was expanded and collimated to fully illuminate the array. The array was placed in the magnified far field of a twelve bit digitizing CCD camera. The output from the camera was captured on a Pentium PC. The data was analyzed off-line in Mathematica.

The CCD was calibrated in the intensity regime pixel by pixel by taking flat field readings from an integrating sphere over a wide range of intensity values. The data was fit to a linear equation that translated pixel level to intensity, which was in turn translated to LRCS per pixel.

The camera was spatially calibrated by acquiring the FFDP's of known circular apertures. A mirror was placed in the array plane and the apertures were inserted between L2 and the flat (see Figure 4). The resulting intensity distributions were captured by the CCD and analyzed off-line. The measured patterns were fit to ideal Airy patterns to generate a scaling parameter. This parameter enabled conversion from pixel number to angle.

IV. Results

The measured time-averaged FFDP of the NRL LEO array is shown in Figure 5 which indicates an approximate Airy distribution and can be compared to Figure 3, which is the modeled pattern. A one-dimensional profile of the modeled and measured data for the time-averaged array can be seen in Figures 6 and 7.

A 21.6% difference between the peak values of the model and the experimental results is apparent in Figure 6. This value is within a precision limit established for the test-bed.

The broadening of the central lobe can be seen as the equivalent of "spoiling" the retroreflectors - a common practice to compensate for velocity aberration. For the orbits of interest, i.e.: the region over 40 micro radians to 50 micro radians, the modeled and measured values agree and indicate that more energy will be distributed in the regions of interest (Figure 7).

Predicted orbital performance using the modeled LRCS with the SLR link equation [3] was then done for Topex passes over Capraia. These results can be seen in Figures 8, 9, and 10. LRCS compared to elevation angle for a high elevation pass is shown in Figure 8. Note that the predicted LRCS is higher at the lower elevation angles ($\sim 10^5$) but still meets the 10^4 criteria at the Point of Closest Approach (PCA). The target was designed this way to compensate for the increased loss due to the R^4 dependence at the longer slant ranges for the lower elevation angles. Predicted number of photoelectrons using the FTLRS for this distribution are shown in Figure 9. The FTLRS uses a telescope that is 13 cm in diameter and is clearly a modest ground station. The predicted response illustrates the capability of the design to close the link.

Predicted LRCS for a low pass (30.54° PCA) over Capraia was also made and is shown in Figure 10. It can be seen in this figure that the 10^4 criterion is met by the array even under these stringent pass conditions.

V. Conclusion

A compact, lightweight retroreflector array was designed, built, and space qualified at the Naval Research Laboratory for low earth orbiting spacecraft. The array consists of 22 one-centimeter fused silica retroreflectors embedded in an aluminum hemisphere 43mm in height, 82 mm in diameter and 221 grams in mass. It was designed to provide a LRCS of at least 10^4 meters squared for typical LEO ranges of 2200 km and lower. The far field diffraction pattern of a single one-centimeter retroreflector was used as the kernel in an incoherent sum approach to produce the time-averaged LRCS of the array.

The FFDP of the array was then characterized in a compact far field optical test bed at NRL. The test bed was calibrated in both the intensity and spatial regime. Results of the characterization showed broadening of the central peak into the side lobes where no null was present. The measured broadening actually enhances the performance of the array for the specific orbits in which it was designed and can be seen as a corollary to "spoiling" the retroreflectors.

The array's predicted orbital performance in terms of LRCS and number of received photoelectrons was then computed for high and low passes over Capraia for a typical TOPEX pass using the Field Transportable Laser Radar System. This predicted performance illustrates the efficacy of the array for LEO orbits using modest SLR ground stations for link closure.

V. References

1. G. Charmaine Gilbreath, Peter B. Rolsma, Robert Kessel, Robert B. Patterson, and James A. Georges III. "Performance Characteristics of a Retroreflector Array Optimized for a LEO Spacecraft", NRL Report 8120--97-9875, December, 1997.
2. G. Charmaine Gilbreath, Peter B. Rolsma, and Robert Kessel. "Analysis of SLR Targets for JASON", NRL Report 8120--97-7971, September, 1997.
3. John J. Degnan, "Millimeter Accuracy Satellite Laser Ranging A Review," Contributions of Space Geodesy to Geodynamics Technology **25**, 133-162 (1993).

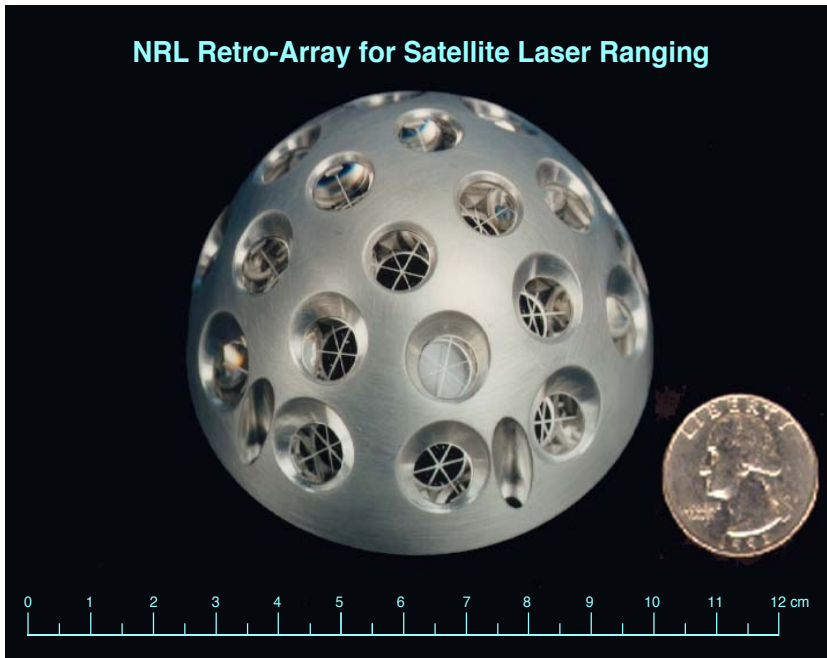


Figure 1. The NRL LEO retroreflector array is illustrated above. The array uses 22 1-cm diameter corner cubes situated on the surface of a 8.2 cm diameter hemisphere and is 221 grams. This array has a field-of-view of 108° and a $\sigma_{\text{LRCS}} \geq 10^4 \text{ m}^2$ for $\theta_{\text{elev}} \geq 20^\circ$.

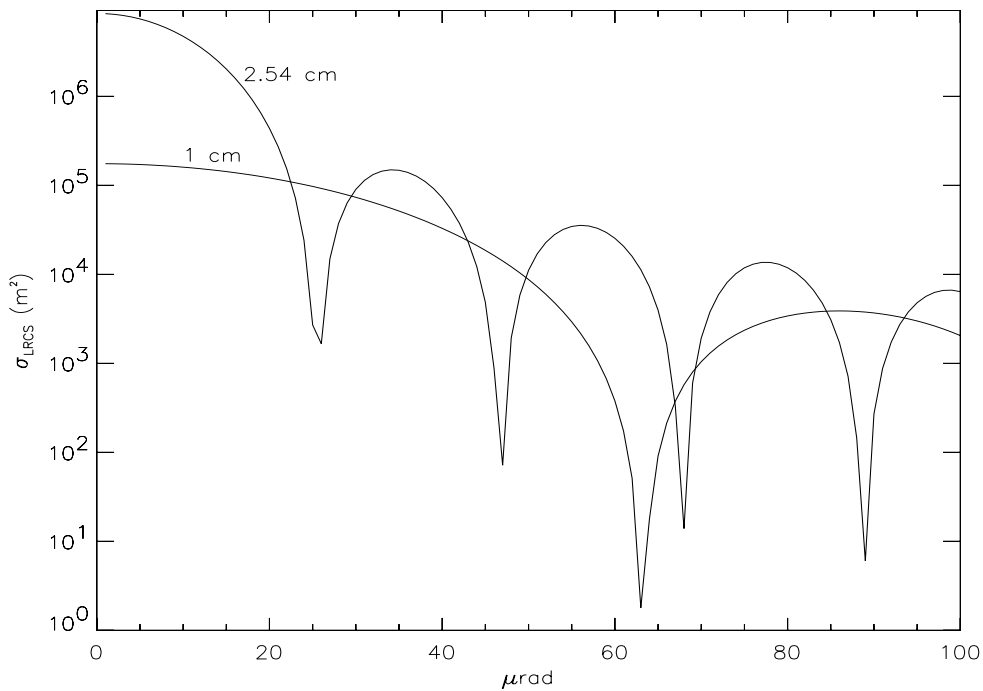


Figure 2. The angular comparison of 1-cm and 2.54-cm diameter retroreflectors' Far Field Diffraction Patterns is shown above.

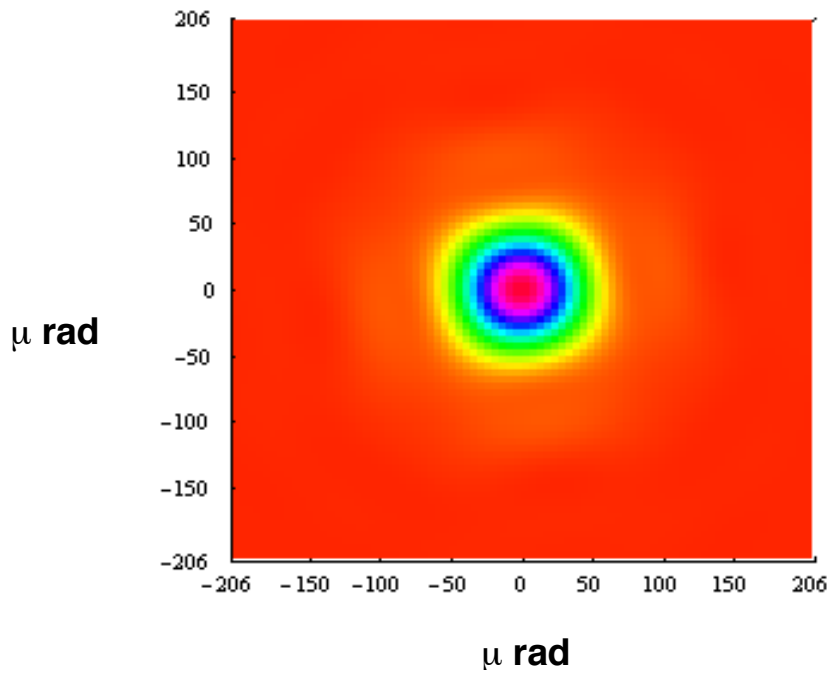


Figure 3. The modeled far field diffraction pattern of the NRL LEO retroreflector for 0..0203 cm bevels and on axis incidence is shown above.

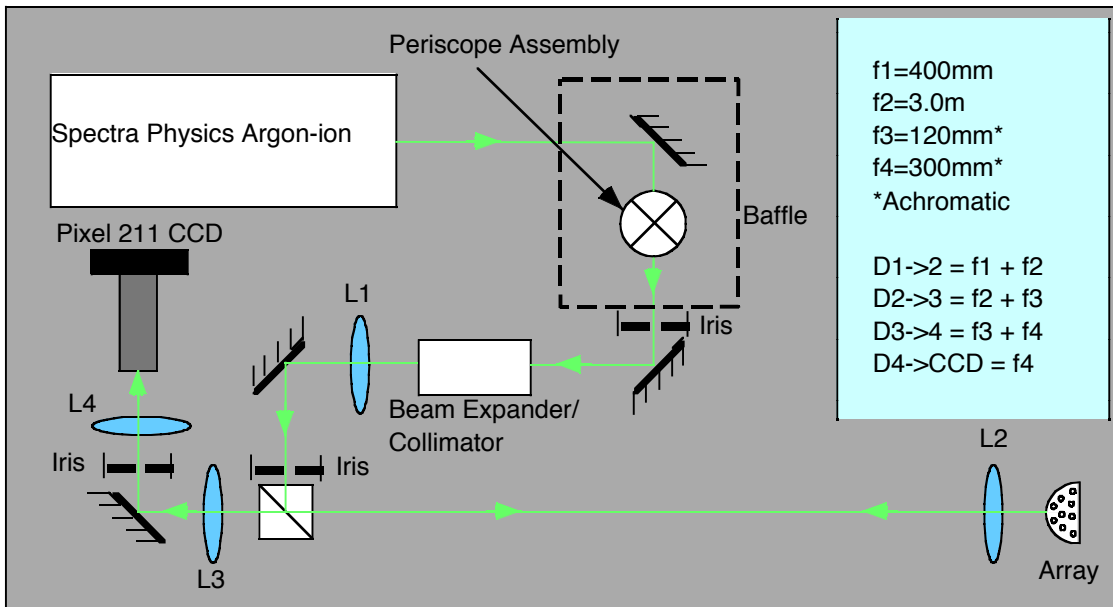


Figure 4. The bench diagram for optical characterization of the NRL LEO array is illustrated.

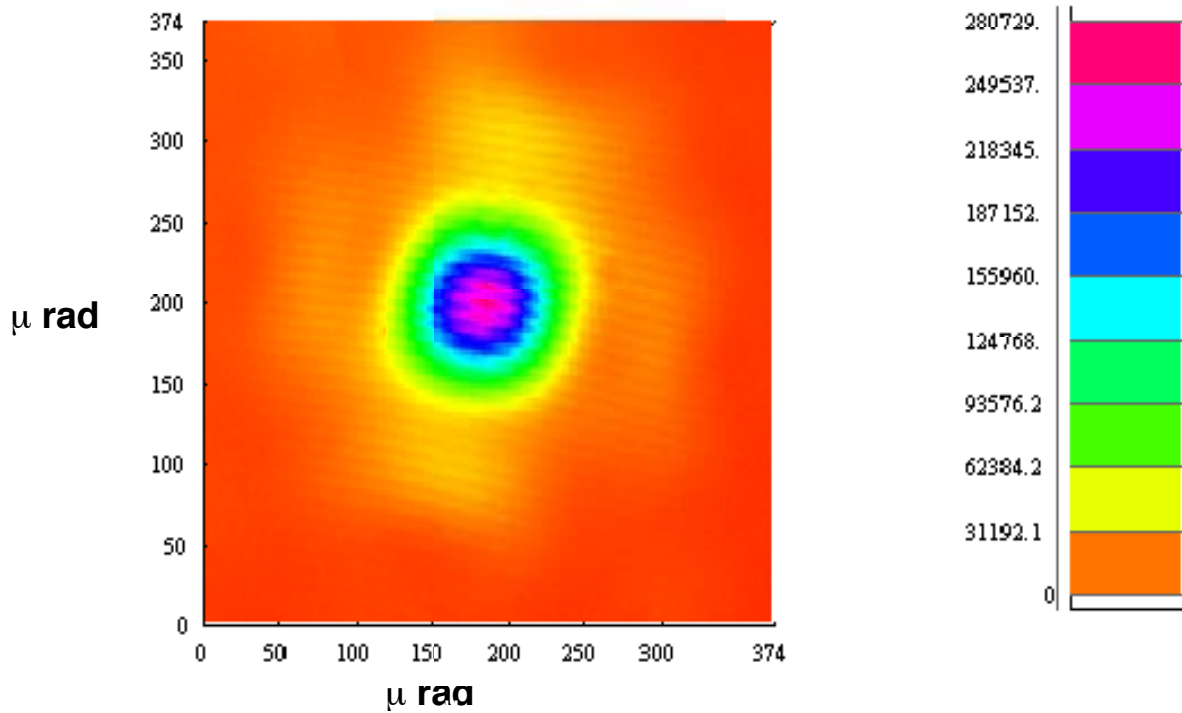


Figure 5. The time-averaged experimental LRCS for the NRL LEO array incidence is shown above.

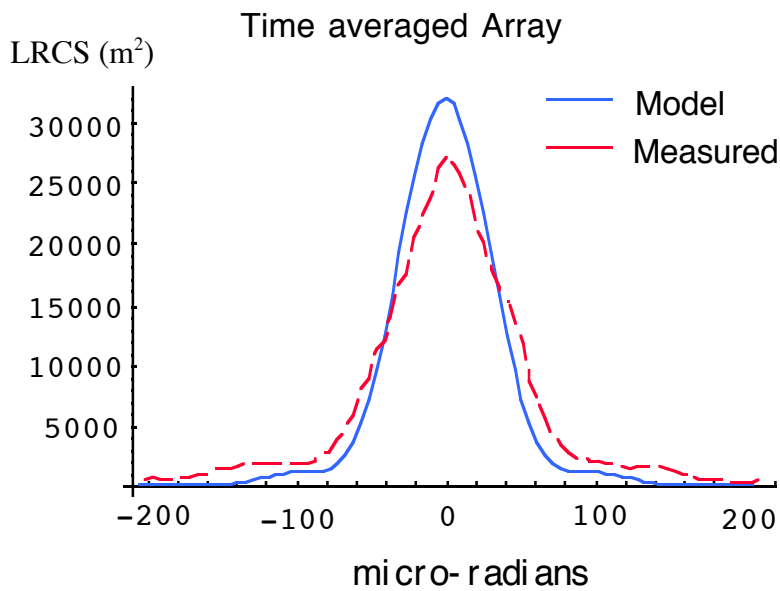


Figure 6. Comparison of modelled LRCS to experimental results for the time-averaged array is shown.

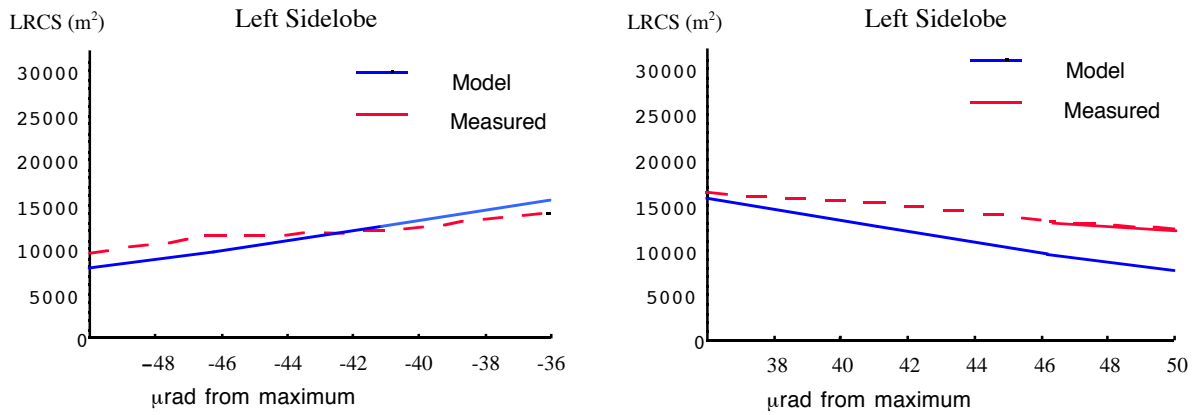


Figure 7: Comparison of side lobe intensities between model and experimental results is plotted above.

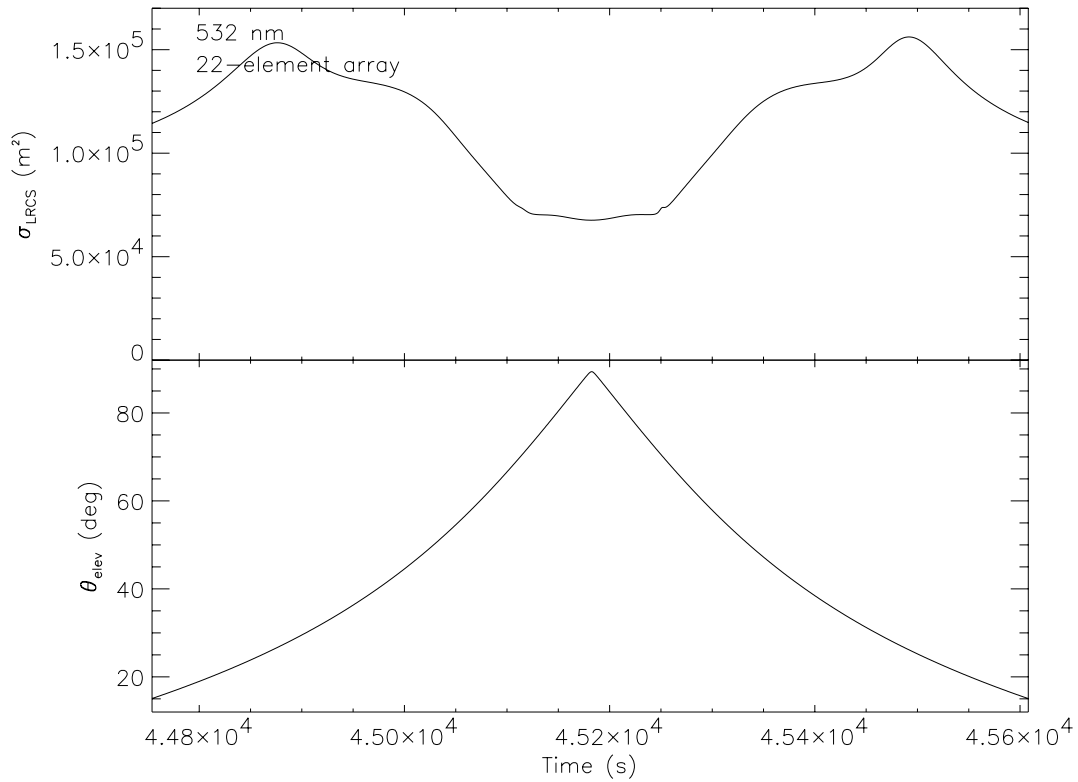


Figure 8. LRCS for a high elevation pass (89.38 deg) is graphed above. Note the larger LRCS at the lower elevation angles.

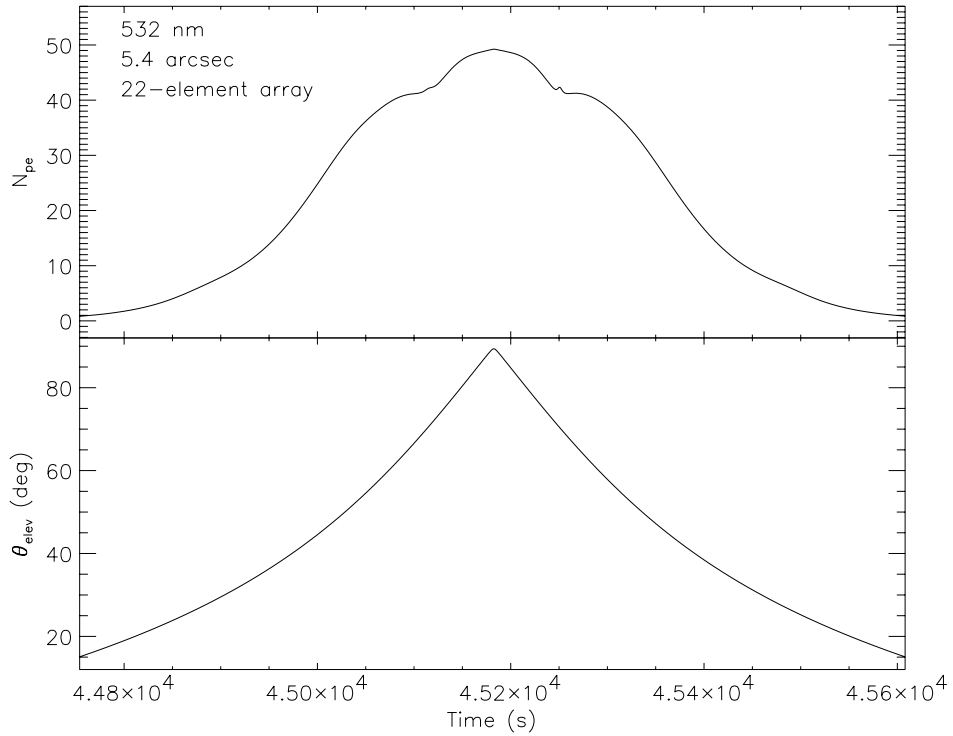


Figure 9. N_{pe} for a high elevation pass (89.38 deg) is shown above. Note that the maximum N_{pe} is predicted at point-of-closest approach.

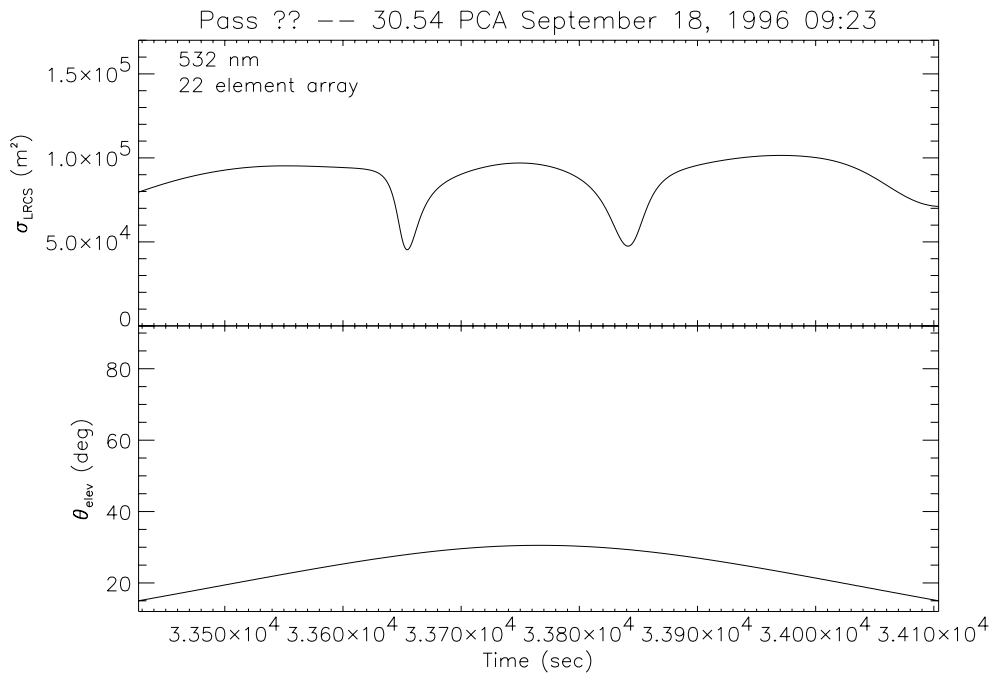


Figure 10. LRCS for a low elevation pass (30.54 deg) is graphed above illustrating that the 10^4 m^2 LRCS requirement is met even for a low pass.